

Supplement of Atmos. Chem. Phys., 18, 3485–3503, 2018
<https://doi.org/10.5194/acp-18-3485-2018-supplement>
© Author(s) 2018. This work is distributed under
the Creative Commons Attribution 4.0 License.



Supplement of

Temporally delineated sources of major chemical species in high Arctic snow

Katrina M. Macdonald et al.

Correspondence to: Greg J. Evans (greg.evans@utoronto.ca)

The copyright of individual parts of the supplement might differ from the CC BY 4.0 License.

S1 Methodology

S1.1 Snow Sample Collection

Arctic snow sampling was completed from September 14th, 2014 to June 1st, 2015, as part of the Network on Climate and Aerosols Research (NETCARE) initiative to create a temporally-refined and broadly speciated dataset of high Arctic snow measurements. Snow samples were collected at Environment and Climate Change Canada's (ECCC) Dr. Neil Trivett Global Atmosphere Watch Observatory at Alert, Nunavut (a remote outpost in the Canadian high Arctic; 82°27' N, 62°30' W). Snow samples were collected from Teflon-surfaced snow tables, two tables each about 1 m² and 1 m above ground level, located about 6 km SSW of the Alert base camp, 201 m above sea level. The tables were located away from the base camp in a minimal traffic site to avoid influences of camp activities. Conditions allowing, samples were collected as soon after the end of each snowfall as feasible. A Teflon scraper and scoop were used to divide the table into rectangular portions for replicate sample collection. The area associated with each sample was recorded. Between sample collections, the tables were fully cleared of any remaining snow and cleaned with methanol. The interval between collections was dependent on snowfall frequency and ranged from 1 to 19 days. Collection bottles, scraper, and scoop were all thoroughly cleaned to avoid contamination.

S1.2 Sample Analysis

Frozen snow samples were analysed in replicate for a broad suite of analytes: BC, major ions, and metals.

Refractory black carbon (BC) was quantified using single-particle soot photometry (SP2). Snow samples collected in 50 mL PYREX bottles were melted rapidly the morning of analysis, and a 50 mL aliquot of each sample was separated into polypropylene vials. After sonication, samples were atomized via Apex-Q nebulizer. The dried particles with 0.02 to 50 fg BC were then quantified via SP2. A quality control standard and analysis blank were analyzed for every batch of 17 samples.

Major ions were measured via ion chromatography (IC). Snow samples collected in 250 mL high-density polyethylene (HDPE) bottles were melted in a warm water bath and analyzed within 3 hours. Analysis was completed using a Dionex IC: DX600 for anions and cations, ICS2000 for organic acids, all using a 200 µL sample loop. Aliquots of these samples were also used for pH analysis (Denver pH analyzer). Equipment was calibrated daily and quality control runs completed every ten samples.

Metals analysis was completed via inductively coupled plasma mass spectrometry (ICP-MS). Samples collected in 500 mL HDPE bottles were melted rapidly in a microwave oven. Sample were immediately filtered with a 0.45 µm cellulose acetate filter to separately quantify the portions of the metals considered as soluble (capable of passing through the 0.45 µm filter) or insoluble (retained by the filter). Both filtrate and filter were digested using 70% nitric acid, ultra-trace grade (SCP Science PlasmaPure). The digestion of the insoluble sample on filters was augmented using a microwave digester (CEM MARS 6). Both filter and filtrate samples were centrifuged and then quantified via ICP-MS (Thermo Scientific iCAP Q). A performance test and calibration (SCP Science PlasmaCAL QC Std 4) were completed prior to each run, and quality control checks were completed

every ten samples. Also, an internal standard was included to quantify and correct for any instrument drift or inter-sample variability (SCP Science Int. Std. Mix 1).

Instrument accuracy was confirmed through the analysis of certified reference materials. Regular analysis of blanks was used for background subtraction and to define method detection limits (MDL) as three standard deviations of the blank levels. Beyond typical preparation blanks, which used DIW in the place of snow melt water, field blanks were also analyzed. Once per month, a set of empty sample bottles was brought to the snow table, opened, and resealed without collection. These field blank bottles were stored and shipped with the regular samples and rinsed with DIW to quantify any contamination throughout the sampling process.

Further details on sampling procedure and analysis are provided in Macdonald et al. (2017).

S2 PMF Seven-Factor Solution

S2.1 Solution Fit

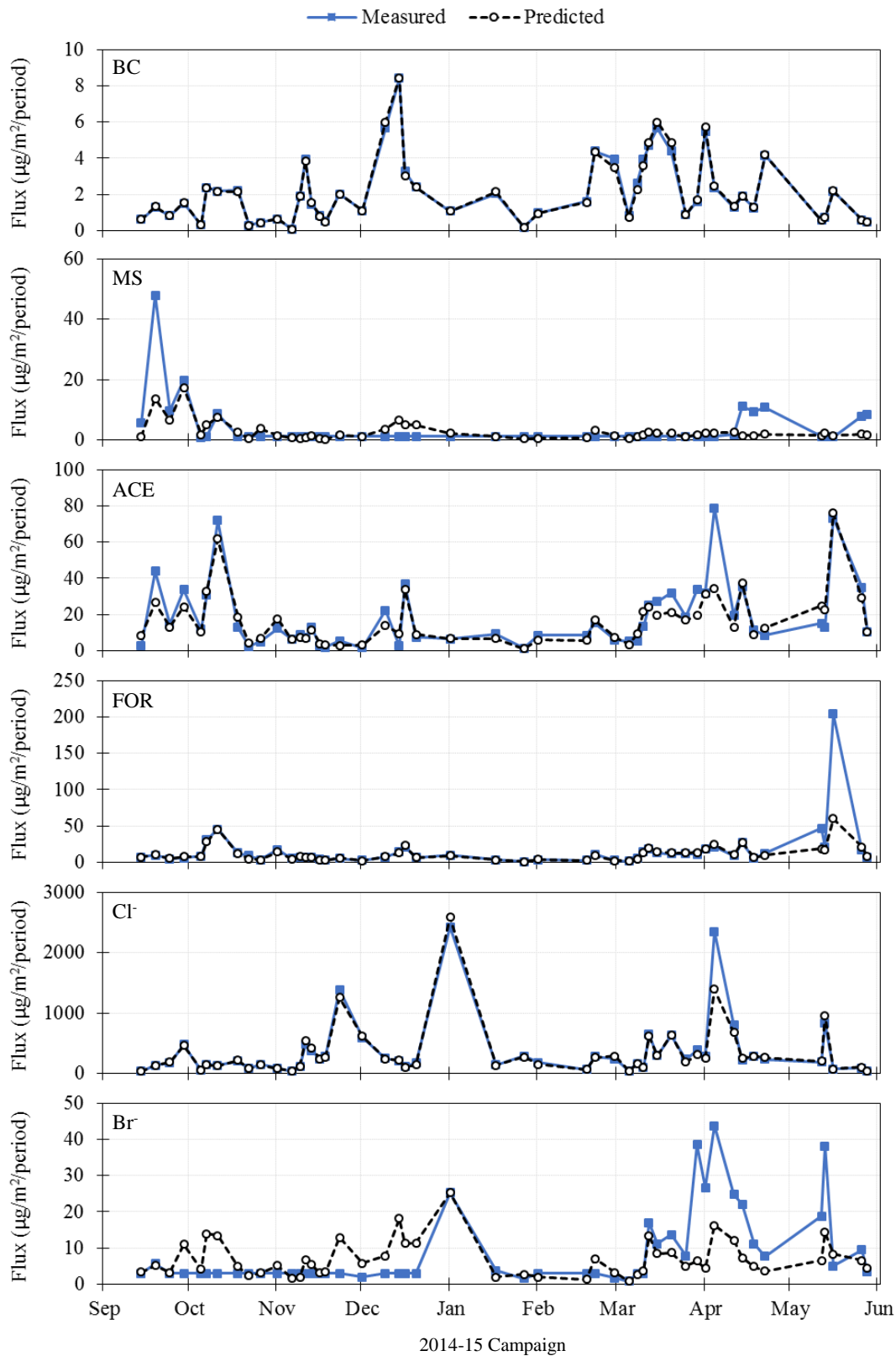


Figure S1: Measured and predicted fluxes of seven-factor PMF solution.

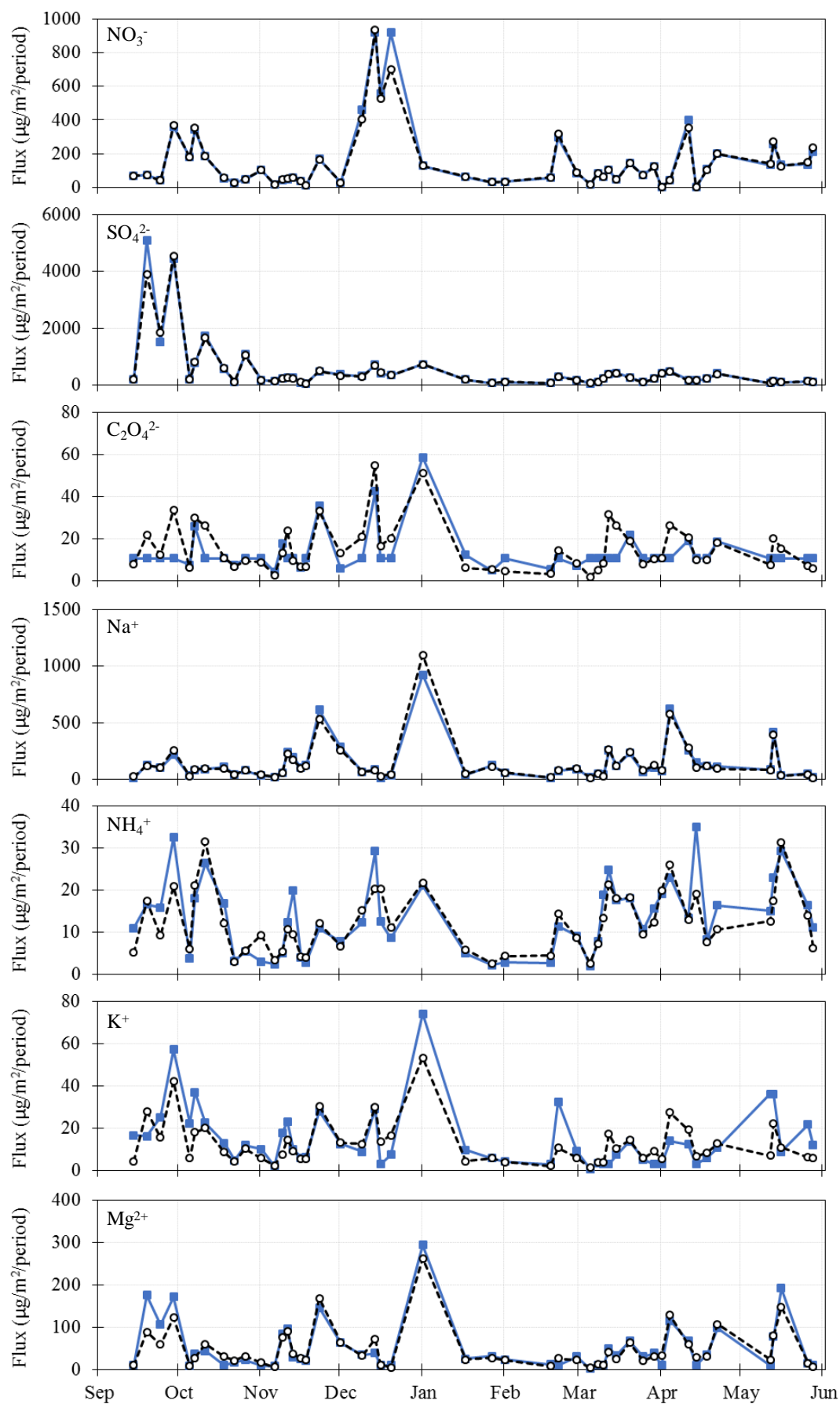


Figure S1 (continued): Measured and predicted fluxes of seven-factor PMF solution.

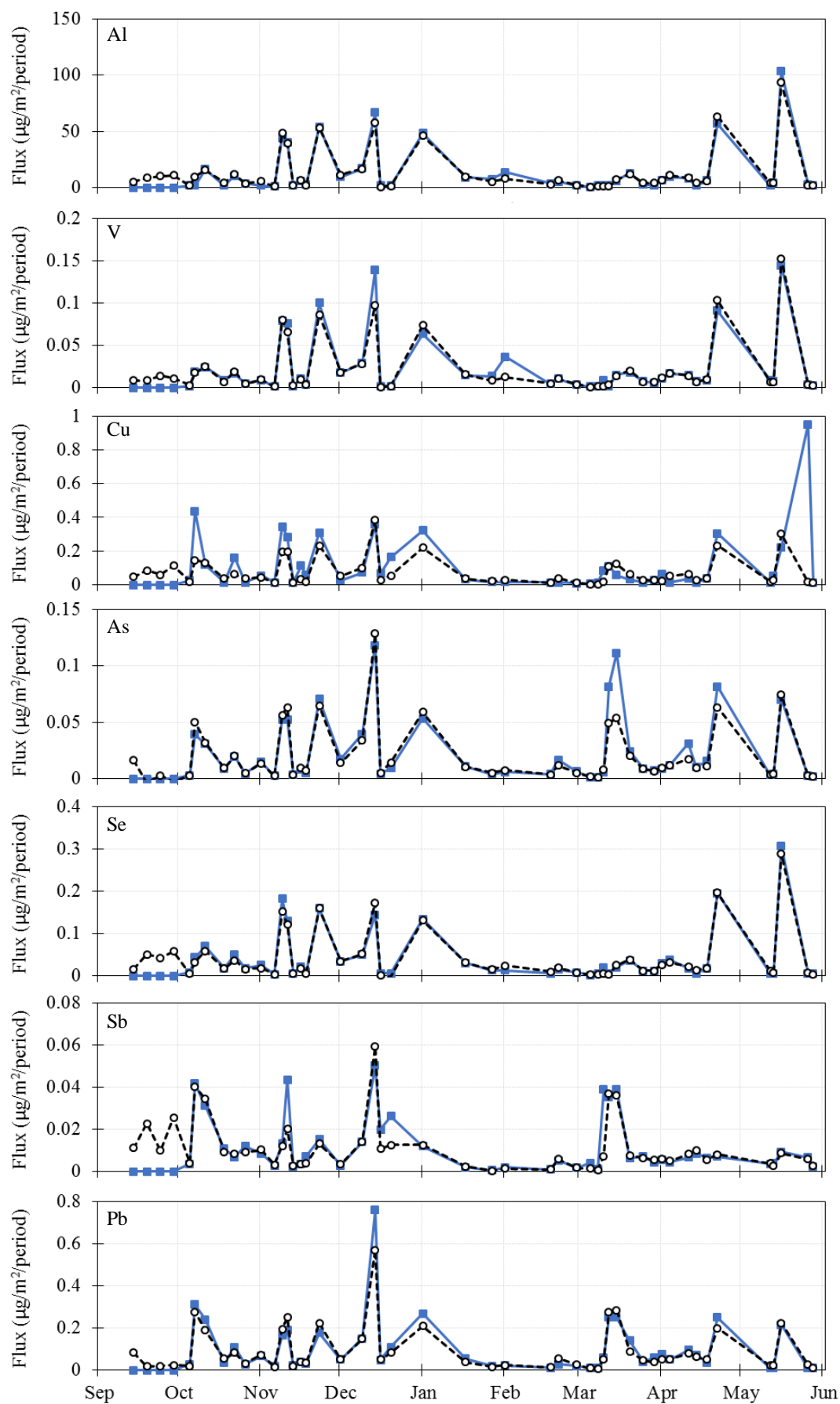


Figure S1 (continued): Measured and predicted fluxes of seven-factor PMF solution.

Notes: All missing values plotted as measured medians.

S2.2 Factor 7 Sulphate FLEXPART Analysis

Volcanic emissions were considered as a possible contributor to Factor 7, sulphate. The heat and speed of a volcanic eruption can potentially increase the emission height substantially. The FLEXPART potential source/influence plots provided in Figure 3 of the manuscript depict back trajectories traced within 500 m of ground level to capture the air masses most likely affected by ground-level sources. Given that a volcanic source could eject particles and gases much higher than this, the specific peak periods for Factor 7 were examined over a larger source altitude range: 0 to 10 km above ground-level. Figure S2 shows the potential source regions for Factor 7 peak periods with this increased source altitude consideration.

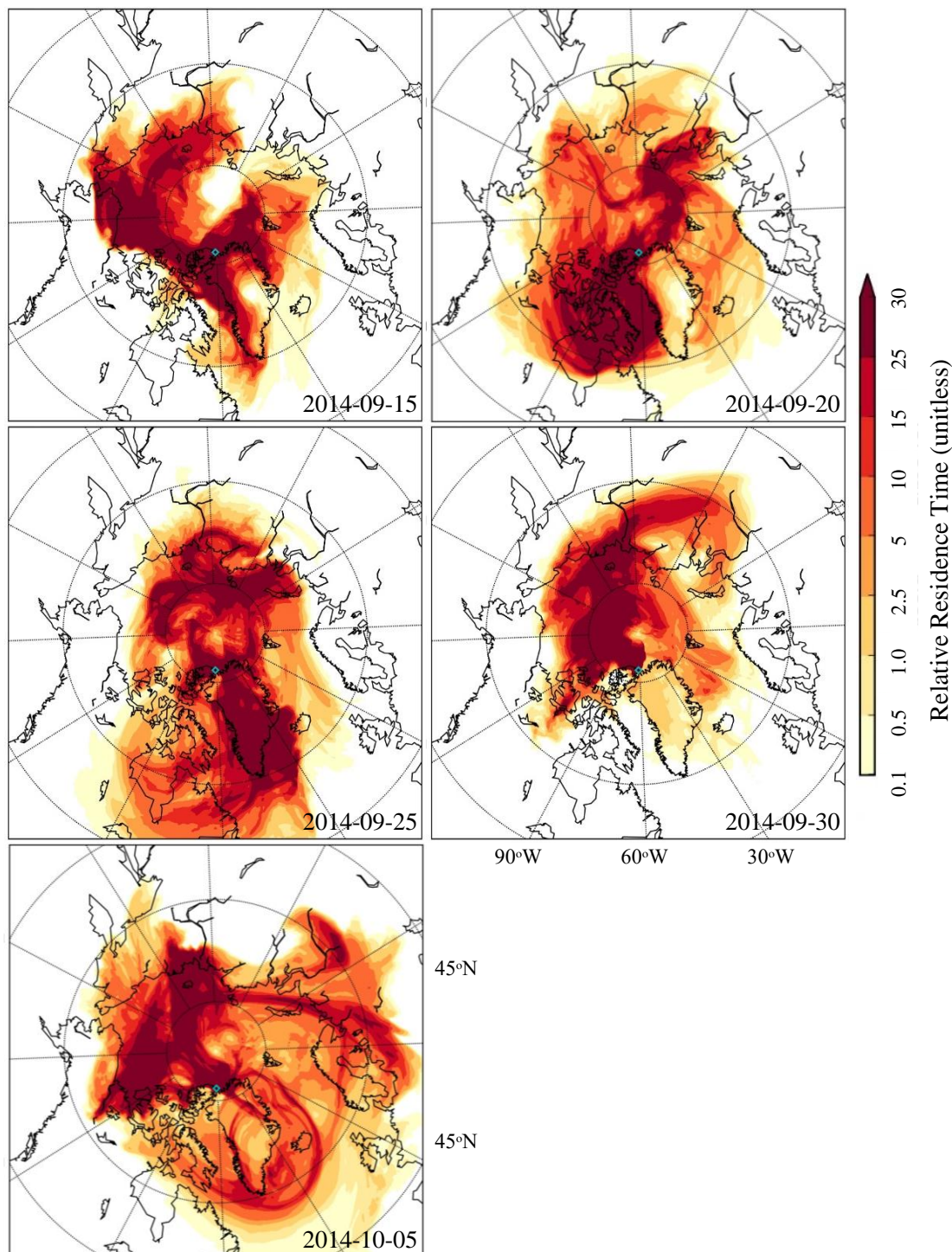


Figure S2: Factor 7, sulphate, peak period 0-10 km potential source region plots.

S2.3 Selection of Optimal PMF Solution

Unlike many other source apportionment methods, PMF offers the distinct advantages of enforced positive factor solutions and weighting of the solution by user-defined uncertainties. This allows realistic interpretation of the solution and the ability to determine the control that individual measurements have over the optimal solution (Norris et al., 2014).

PMF solution optimization is described using the Q-value, as described in Eq. 3 in the manuscript. The Q value can be calculated via two different modes: true (Q_{true}) or robust (Q_{rob}). These modes are identical except that the robust mode of analysis excludes measurements from the calculation of Q if they have a e_{ij}/u_{ij} value greater than 4 (where e_{ij} and u_{ij} are defined as described in Eq. 3); thus, the robust mode reduces the impact of outliers. The robust mode was used for this analysis as it is better suited for environmental data which may not be normally distributed (Norris et al., 2014).

Selection of the number of factors is a critical step of a PMF analysis. Trial runs ranging from 2 to 9 factors were completed using 100 distinct random seeds per run. This study used five considerations during the selection of an optimal number of factors. Firstly, the improvement in Q_{rob} observed with the addition of a factor was calculated. The addition of another factor should improve the calculated Q_{rob} value to be considered a viable factor. Secondly, the solution's Q_{rob} was compared to the expected value of Q, calculated as follows (Norris et al., 2014):

$$Q_{\text{exp}} = nm - (pn + pm) \quad , \quad (\text{S1})$$

where Q_{exp} is the expected value of Q, n is the number of measurements, m is the number of analytes, and p is the number of factors.

A ratio of Q_{rob} to Q_{exp} of one was considered ideal. Thirdly, the reproducibility of the solution was examined such that solutions with greater reproducibility among the 100 seeded calculations for each run were given more consideration. Fourthly, the fit of each potential solution was considered. The residuals of each analyte were examined for each potential solution to ensure that they were normally distributed and with a minimal number of normalized residual values greater than 3 across all samples and analytes. Also, the correlation of predicted and measured values was calculated for all analytes. Finally, the interpretability of each solution was considered. Only solutions which produced factor profiles which could be explained in a real-world setting were considered.

Based on the criteria outlined above, the seven-factor solution was found to be optimal. The seven-factor solution produced one of the largest Q_{rob} improvements with the addition of a factor, an acceptable $Q_{\text{rob}}/Q_{\text{exp}}$ value, and good reproducibility. In particular, the seven-factor solution showed a marked improvement in fit and interpretability over solutions with fewer factors. The seven-factor solution reproduced measurements with a Pearson's correlation coefficient above 0.8 for all strong analytes. The four, six, and seven-factor solutions all provided readily interpretable source profiles, but the seven-factor solution was considered the most realistic. Furthermore, a repeat run using 500 seeds showed the seven-factor solution to be consistent and stable. Figure S3 described the evolution of the PMF solution composition from 2 to 9 factors. Figure S4 provides key metrics used to evaluate the optimal number of factors.

The final solution statistics were: $Q_{\text{rob}} = 355$, $Q_{\text{exp}} = 329$, $Q_{\text{rob}}/Q_{\text{exp}} = 1.08$, stability = 94%, and median predicted/measured correlation = 0.94.

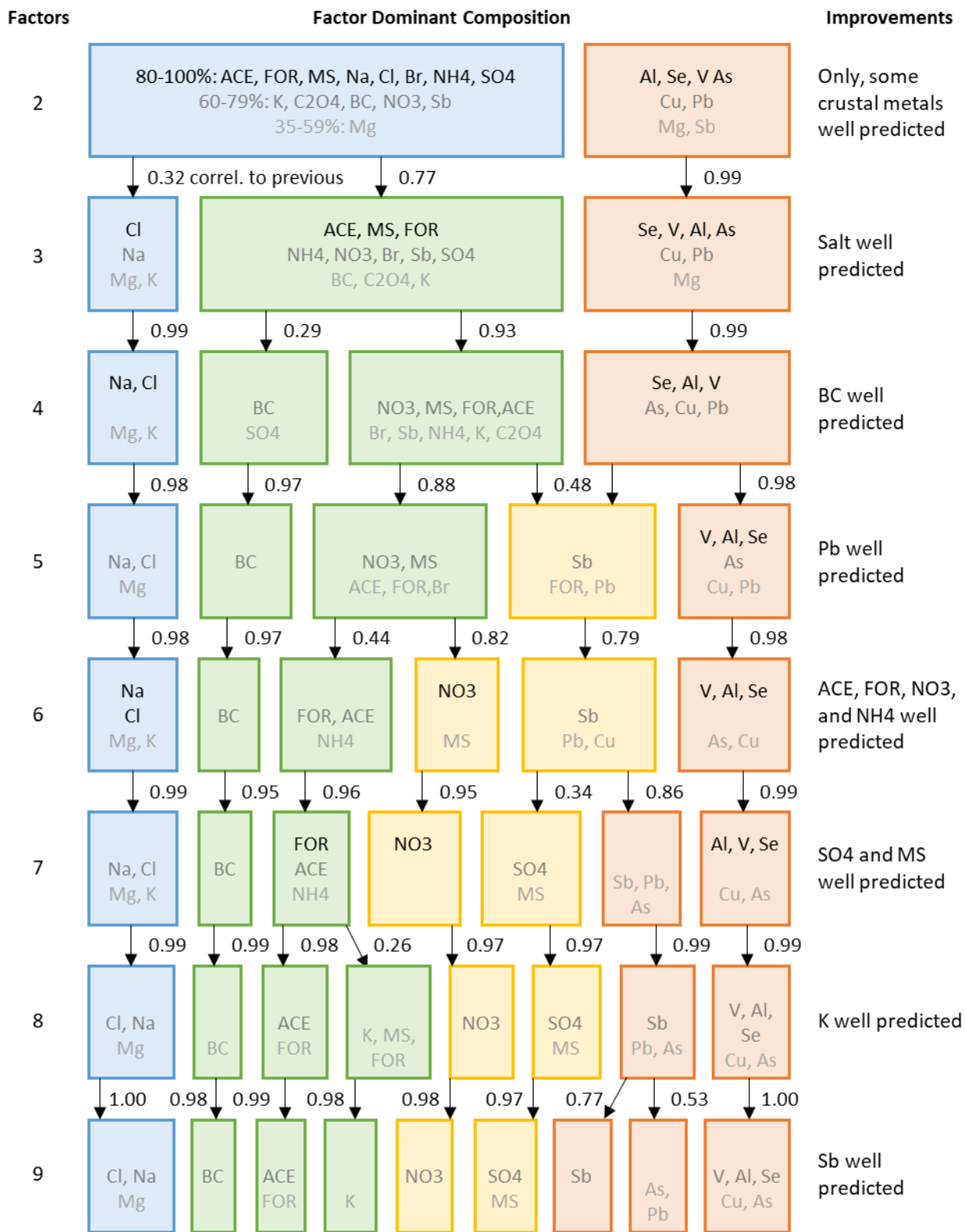


Figure S3: Evolution of factor composition of 2 to 9-factor PMF solutions.

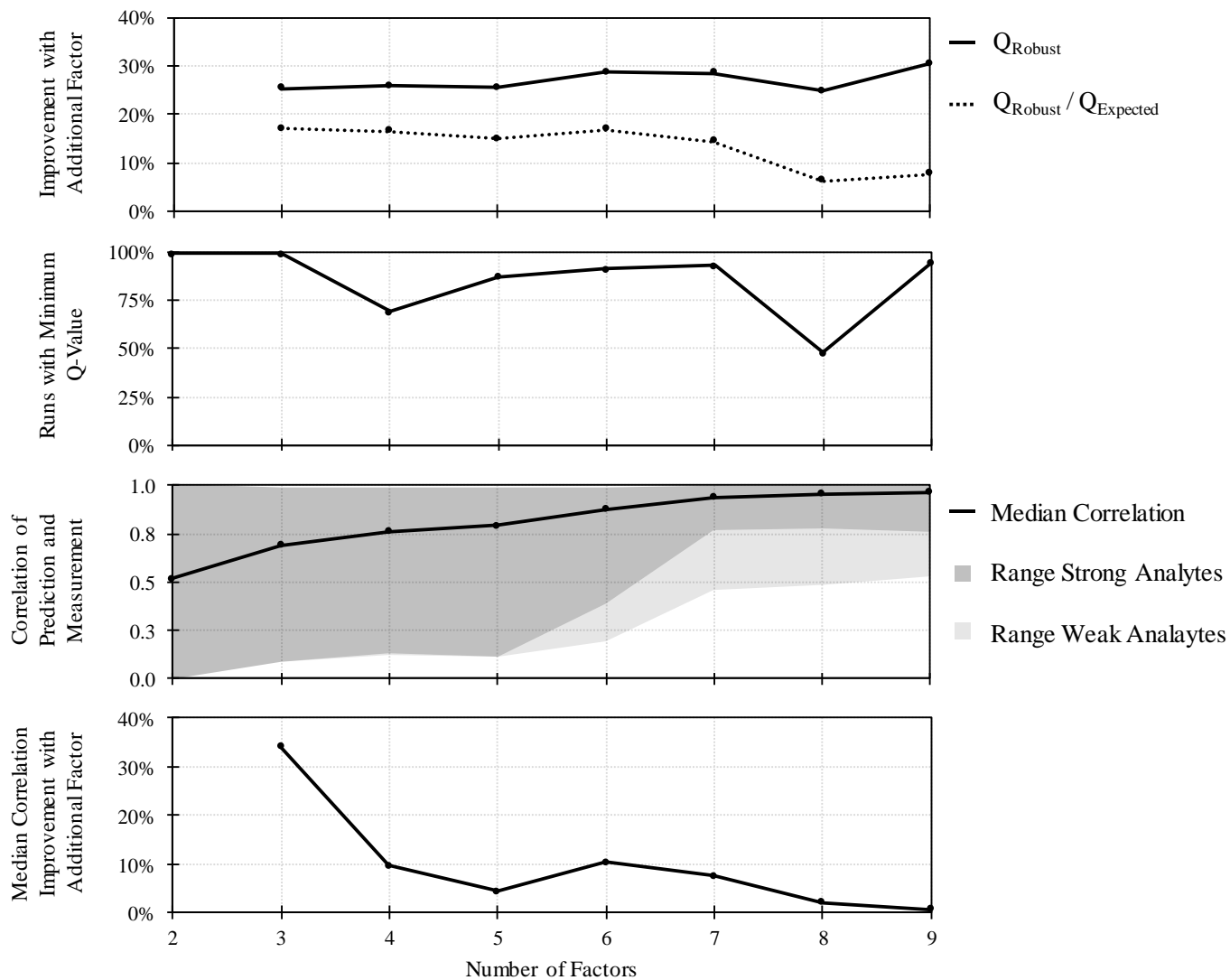


Figure S4: PMF Flux per Period Solution Parameters across the Number of Factors Used. Agreement of measurements and PMF prediction: line depicts median Pearson's correlation coefficient, dark shaded area depicts range of correlations for strong analytes and light shaded area range for weak analytes.

S3 Alternative PMF Solutions

S3.1 Concentration and Flux per Day PMF Analyses

Three metrics were considered as the basis for this analysis: analyte concentration, flux per day, and flux per snowfall (i.e., assuming each sample represented a single snowfall event regardless of the time period over which it occurred, which is known to be true for the majority of samples based on Alert station operator records). Identical PMF analyses were completed for all three metrics, and it was found that the factor profiles identified by all three metrics showed excellent agreement, with Pearson's correlation coefficients above 0.95 for all factors; however, factor contributions varied across the metrics, with correlations as low as 0.35. This is as expected, since the relative variation between analytes does not change with the use of different snow metrics, but the time series should change given that the metrics represent different physical phenomena. Snow flux per snowfall period results are provided in the manuscript while concentration and flux per day results are available in Table S1 and S2.

Table S1: Factor compositions based on different snow metrics.

Metric	Snow Concentration							Snow Flux per Day						
	1	2	3	4	5	6	7	1	2	3	4	5	6	7
BC	5	0	66	17	0	8	5	4	0	55	15	3	15	7
MS	5	0	10	12	27	4	42	7	0	18	7	30	0	39
ACE	0	5	10	79	0	0	6	2	7	7	79	0	0	5
FOR	0	10	0	80	1	8	0	3	11	0	80	0	7	0
Cl⁻	79	3	7	2	2	2	5	75	2	5	6	3	4	6
Br⁻	33	0	0	26	23	15	4	32	0	0	29	20	15	4
NO₃⁻	0	10	4	0	86	0	0	3	8	2	1	79	0	6
SO₄²⁻	9	4	5	0	4	9	68	10	0	5	0	4	15	67
C₂O₄²⁻	27	8	9	8	14	22	12	25	11	7	5	15	22	15
Na⁺	79	4	0	2	0	7	9	75	2	0	7	0	8	8
NH₄⁺	15	2	17	47	5	5	8	16	2	13	49	6	7	8
K⁺	38	10	0	4	20	10	19	38	7	0	7	19	11	18
Mg²⁺	43	34	1	5	0	0	17	46	30	1	8	0	0	15
Al	2	84	0	0	3	3	7	3	88	0	0	3	1	4
V	2	84	1	1	3	5	5	3	87	1	1	3	5	2
Cu	6	48	0	0	7	28	11	6	45	0	0	7	33	9
As	5	44	7	0	0	44	0	4	40	7	0	2	48	0
Se	0	81	2	1	0	3	12	0	85	2	0	0	3	9
Sb	0	0	4	18	1	60	17	0	0	4	19	2	60	15
Pb	4	25	8	8	0	53	2	3	21	8	7	0	57	3
Fit with Flux/Period	0.99	0.99	0.97	0.99	0.99	0.98	0.99	1.00	1.00	0.98	0.99	1.00	0.99	0.99

Notes: Pearson's correlation coefficients provided for fit with flux/period solution

The source contributions identified by the flux per snowfall period analysis were the most readily interpreted as physically realistic factors. Moreover, this metric showed the largest correlation between BC snow and atmospheric measurements (Pearson's correlation coefficients of 0.4, 0.3, and 0.5 for BC concentration, flux per day, and flux per snowfall period, respectively), implying that the flux per snowfall may in general be more closely related to the change in analyte sources over time while concentration and flux per day may be more intrinsically dependent on changes in deposition processes. For example

flux per snowfall is likely related to a specific synoptic event, arising from a common location. This will be more useful than concentration given that this value will be affected by the amount of precipitation, and more useful than flux per day that will be affected by the rapidity of snowfall.

Table S2: Factor contributions based on different snow metrics.

Metric	Snow Concentration							Snow Flux per Day						
Factor	1	2	3	4	5	6	7	1	2	3	4	5	6	7
mm-dd	2014													
09-14	0.0	0.4	0.1	0.6	0.5	1.4	0.3	0.0	0.3	0.3	1.0	0.9	0.9	0.9
09-19	-0.2	-0.2	-0.2	1.1	0.6	-0.2	11.4	-0.2	0.5	-0.2	0.3	-0.2	-0.2	4.7
09-24	0.3	0.5	0.0	0.5	0.3	-0.2	5.3	0.9	-0.2	-0.1	1.6	-0.2	-0.2	16.5
09-29	0.9	-0.2	-0.1	0.8	2.8	-0.2	13.1	0.1	0.3	-0.2	0.2	0.5	-0.2	4.9
10-05	0.1	0.1	0.0	0.8	1.4	0.2	0.4	0.1	0.1	-0.1	0.6	1.2	0.2	0.5
10-07	0.1	0.5	0.4	2.3	2.6	5.0	1.5	-0.2	2.2	-0.2	5.9	7.5	13.5	4.5
10-11	0.0	0.9	-0.2	4.2	1.3	2.7	4.4	-0.1	0.4	-0.1	1.3	0.3	0.8	1.7
10-18	0.6	0.2	1.0	1.1	0.4	0.6	1.5	0.3	0.2	0.7	0.5	0.1	0.2	0.9
10-22	0.2	1.0	0.0	0.2	0.1	1.2	0.1	0.1	0.8	-0.1	0.1	0.1	0.8	0.1
10-26	0.3	0.0	-0.1	0.3	0.4	0.5	3.0	0.2	0.2	-0.2	0.2	0.1	0.3	3.1
11-01	0.2	0.4	0.0	1.3	0.7	1.1	0.3	0.2	0.8	-0.2	1.9	1.2	1.7	0.6
11-06	0.1	0.0	-0.1	0.5	0.2	0.2	0.3	0.1	0.1	-0.2	0.5	0.2	0.3	0.5
11-09	0.1	4.3	1.1	0.1	-0.2	1.7	0.1	0.2	4.5	1.1	-0.1	-0.2	1.4	0.3
11-11	1.6	3.5	2.3	0.0	-0.1	3.0	-0.2	2.3	5.6	3.6	-0.2	-0.2	3.9	-0.2
11-13	1.4	0.1	0.8	0.7	0.4	0.0	0.4	1.9	0.1	1.4	0.8	0.4	0.0	0.7
11-16	0.8	0.5	0.4	0.2	0.2	0.4	0.0	0.7	0.5	0.4	0.1	0.2	0.3	0.1
11-18	1.0	0.2	0.2	0.2	0.1	0.5	0.0	1.3	0.2	0.3	0.2	0.1	0.6	-0.1
11-23	4.4	4.6	0.9	-0.2	0.7	2.0	0.2	1.7	2.1	0.4	-0.2	0.2	0.7	0.2
12-01	2.2	0.9	0.5	0.1	0.1	0.3	0.5	1.3	0.6	0.4	0.0	0.0	0.2	0.4
12-09	0.4	1.3	3.9	0.5	2.7	1.7	0.1	0.1	0.6	1.8	0.1	1.1	0.6	0.1
12-14	-0.2	4.6	5.1	-0.2	6.3	8.7	-0.2	-0.2	4.8	4.3	-0.2	5.9	7.1	-0.2
12-16	0.1	-0.2	1.4	2.3	4.0	0.5	0.9	-0.2	-0.2	2.3	2.9	5.6	0.5	1.4
12-20	0.2	-0.2	1.4	0.5	5.3	1.5	0.4	0.1	-0.1	0.7	0.3	2.9	0.7	0.2

Table S2 (continued): Factor contributions based on different snow metrics.

Metric	Snow Concentration (continued)							Snow Flux per Day (continued)						
	1	2	3	4	5	6	7	1	2	3	4	5	6	7
mm-dd	2015													
01-01	9.4	3.8	-0.2	0.3	0.5	1.8	0.3	9.5	4.4	-0.2	-0.2	0.1	1.7	0.6
01-17	0.3	0.8	1.4	0.3	0.3	0.1	0.3	0.1	0.3	0.6	0.1	0.1	0.0	0.2
01-27	1.0	0.4	0.1	0.1	0.2	0.0	0.0	0.4	0.2	0.0	0.0	0.1	0.0	0.0
02-01	0.5	0.7	0.5	0.3	0.2	0.0	0.2	0.4	0.7	0.6	0.2	0.1	0.0	0.2
02-18	0.1	0.3	1.0	0.3	0.4	0.0	0.1	0.3	0.7	3.2	0.6	1.0	-0.2	0.3
02-21	0.6	0.4	2.8	0.9	2.2	0.3	0.4	0.3	0.3	1.8	0.4	1.2	0.1	0.2
02-28	0.8	0.1	2.3	0.2	0.5	0.0	0.2	0.3	0.0	0.9	0.1	0.2	0.0	0.1
03-05	0.1	0.0	0.5	0.2	0.1	0.1	0.1	0.1	0.1	0.8	0.2	0.2	0.1	0.2
03-08	0.4	0.0	1.5	0.5	0.6	-0.2	0.2	0.4	0.0	1.7	0.4	0.5	-0.2	0.2
03-10	0.1	0.0	2.1	1.3	0.4	0.5	0.4	0.1	0.0	3.8	1.7	0.5	0.6	0.6
03-12	1.9	-0.2	2.4	1.5	0.7	5.0	0.0	2.3	-0.2	3.3	1.7	0.9	5.9	-0.2
03-15	0.6	0.4	3.4	1.0	0.1	4.9	0.2	0.5	0.5	3.4	0.8	0.1	3.9	0.0
03-20	2.0	1.0	2.9	1.2	0.8	0.6	0.1	0.8	0.4	1.5	0.4	0.3	0.2	0.1
03-25	0.6	0.3	0.2	1.2	0.5	0.6	0.1	0.4	0.3	0.2	0.7	0.3	0.4	0.1
03-29	1.0	0.2	0.8	1.3	0.9	0.2	0.4	0.8	0.3	0.9	1.0	0.7	0.2	0.4
04-01	0.6	0.5	3.5	1.8	-0.2	-0.1	0.9	0.3	0.4	3.1	1.1	-0.2	-0.1	0.7
04-04	5.0	0.8	0.7	2.4	0.2	-0.2	0.6	7.1	1.3	1.9	2.8	-0.1	-0.2	1.1
04-11	2.4	0.6	0.5	0.9	2.6	1.0	-0.2	1.2	0.4	0.2	0.4	1.4	0.5	-0.1
04-14	0.8	0.3	0.5	2.7	0.0	0.6	0.2	0.9	0.5	1.2	3.5	-0.2	0.9	0.4
04-18	0.9	0.4	0.6	0.6	0.7	0.6	0.3	0.9	0.5	0.7	0.4	0.7	0.5	0.4
04-22	0.5	5.6	2.8	0.2	0.7	0.9	0.4	0.5	6.1	3.2	-0.1	0.7	0.7	0.7
05-12	0.7	0.3	-0.1	1.9	1.0	0.0	0.0	1.9	1.1	-0.1	5.3	3.4	0.0	0.3
05-13	3.5	0.2	-0.2	1.7	2.0	-0.1	-0.2	9.0	0.6	-0.2	3.7	5.3	-0.2	-0.2
05-16	-0.2	8.5	0.3	5.2	0.0	-0.2	-0.2	-0.2	5.1	0.4	2.3	-0.1	-0.1	0.2
05-26	0.3	0.1	-0.2	2.2	1.1	0.1	0.3	0.2	0.2	-0.2	2.7	1.6	0.1	0.5
Fit Flx/Per	0.82	0.88	0.60	0.69	0.69	0.74	0.82	0.87	0.90	0.83	0.65	0.75	0.82	0.60

Notes: Pearson's correlation coefficients provided for fit with flux/period solution

S3.2 Four and Six-Factor PMF Solutions

The four-factor PMF solution is described below (Figure S5). Factors 1, 2, and 3 were practically identical to their counterparts in the seven-factor solution. Factor 4 of the four-factor solution was found to be characterized by several major ions, fall/spring peaks, and local Arctic source areas. Thus, Factor 1 was identified as a sea salt source, Factor 2 as a crustal source, Factor 3 as a combined long-range transport source, and Factor 4 as a mixture of aged transported emissions and local emissions.

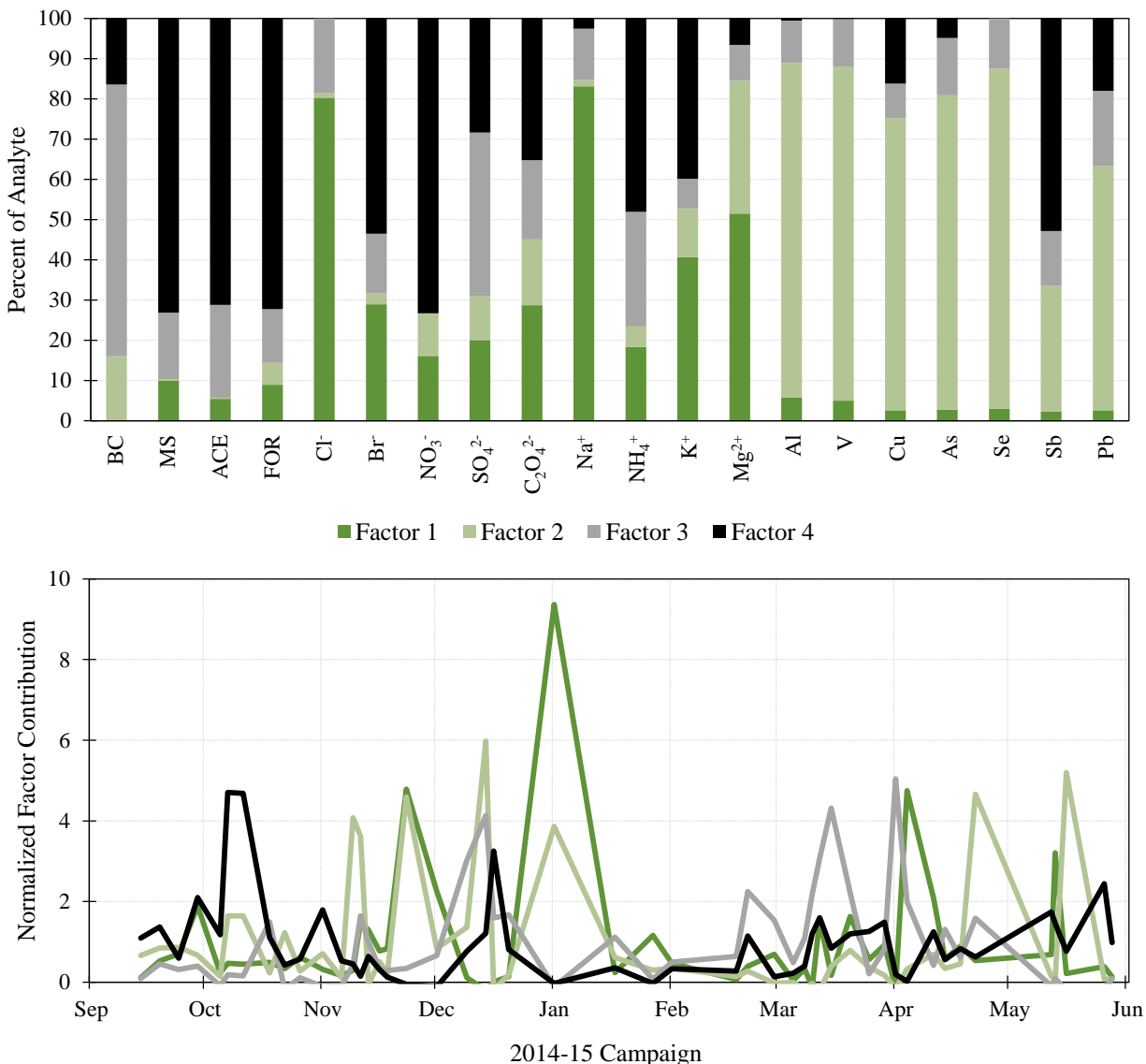


Figure S5: Four-factor PMF solution: Factor compositions and contributions.

The six-factor PMF solution is described below (Figure S6). The six-factor solution was found to be essentially identical to that of the seven-factor solution, with the exception that Factors 6 and 7 of the seven-factor solution combined to form Factor 6 of the six-factor solution. As discussed in section 3.2.7 in the main text, this new Factor 6 was not as readily interpretable as the split factors. The six-factor solution however provided the largest improvement in Q values and prediction accuracy with the addition of a factor, thus was included here as a potential solution.

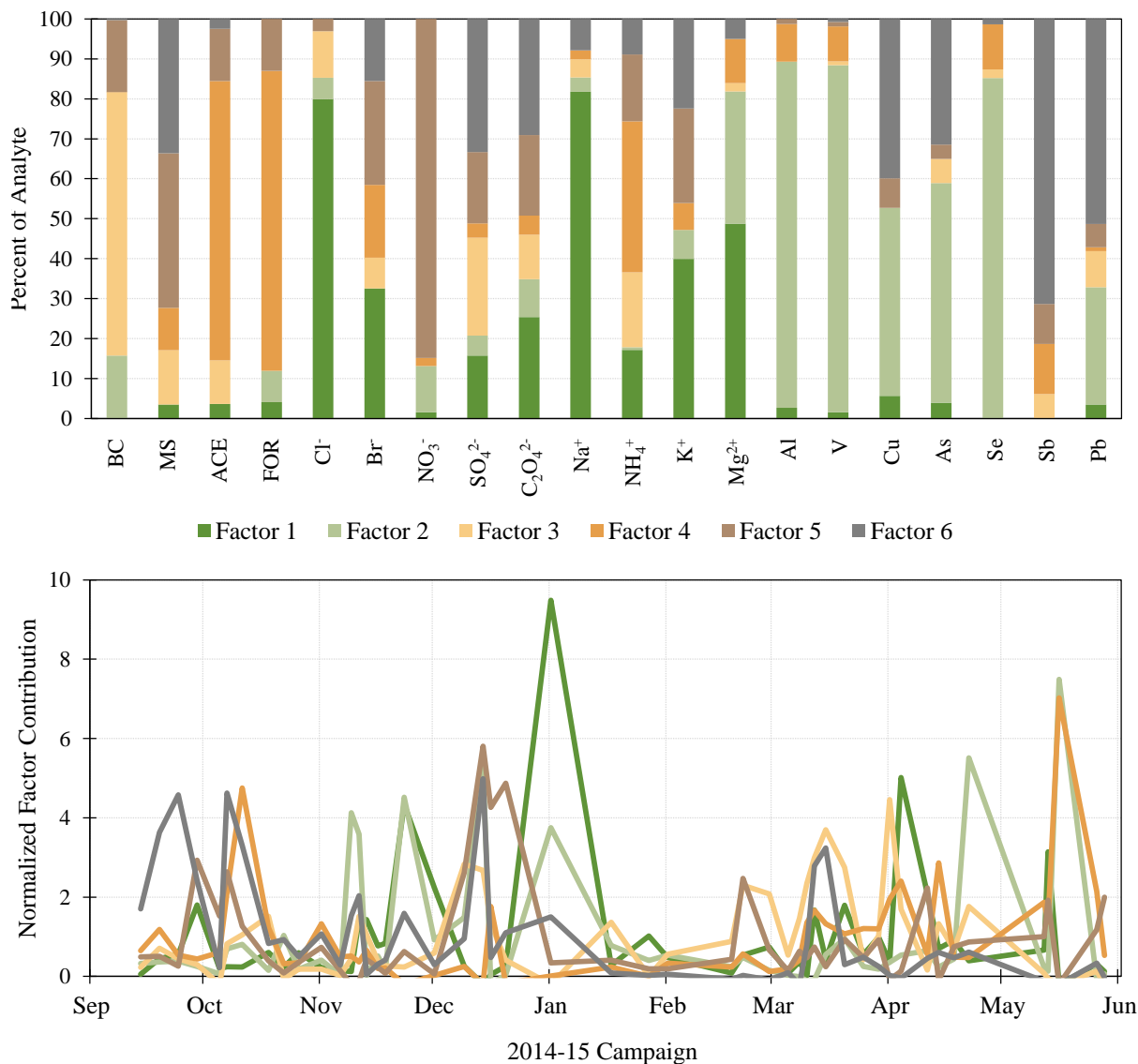


Figure S6: Six-factor PMF solution: Factor compositions and contributions.

Diagnostic parameters for the four and six-factor PMF solutions are provided in table S3. The seven-factor solution showed improved prediction relative to both the four and six-factor solutions, as demonstrated by comparison of Table S3 to Table 1 in the manuscript. Most notably, the predicted fit for the following analytes was greatly improved from the four-factor solution to the seven factor solution: acetate, formate, NO₃⁻, SO₄²⁻, NH₄⁺, insoluble Sb, MS, and Br⁻. Residuals of these analytes were also improved, as were the residuals for BC, Mg²⁺, insoluble Al, Se, Sb and Pb. The six-factor solution showed good prediction for most analytes; however, inclusion of the seventh factor improved prediction of SO₄²⁻, Mg²⁺, and MS. The seven-factor solution also improved the residuals of these analytes as well as BC, NO₃⁻, insoluble Al, and Se compared to the six-factor solution. Specifically, the six-factor solution did not predict the distinct measured fall peaks in SO₄²⁻ nor the measured moderate fall peaks in MS. A comparison of the predicted and measured SO₄²⁻ flux for the six-factor solution is provide in Figure S7.

Table S3: Diagnostic properties of four and six-factor solutions.

Analyte	Four-Factor Solution			Six-Factor Solution		
	Predicted/ Measured Fit	Normalized Residual Mean	Normalized Residual Deviation	Predicted/ Measured Fit	Normalized Residual Mean	Normalized Residual Deviation
Strong Analytes						
BC	0.97	0.07	0.59	0.99	0.02	0.32
ACE	0.51	0.21	1.16	0.86	0.10	0.89
FOR	0.21	0.33	1.24	0.89	0.12	0.77
Cl ⁻	0.96	0.03	0.49	0.96	0.04	0.48
NO ₃ ⁻	0.37	0.72	1.67	0.98	0.02	0.34
SO ₄ ²⁻	0.13	0.58	1.41	0.38	0.47	1.32
Na ⁺	0.99	0.03	0.48	0.98	0.02	0.40
NH ₄ ⁺	0.65	0.14	0.87	0.83	0.08	0.67
K ⁺	0.74	0.24	1.09	0.74	0.25	1.12
Mg ²⁺	0.82	0.10	0.73	0.85	0.08	0.66
Al	0.94	0.04	0.69	0.99	0.02	0.48
V	0.96	0.13	0.82	0.98	0.11	0.60
As	0.80	0.19	0.98	0.86	0.12	0.94
Se	0.92	0.06	0.63	0.99	0.03	0.51
Sb	0.68	0.55	1.61	0.89	0.14	0.96
Pb	0.85	0.16	1.04	0.95	0.02	0.74
Weak Analytes						
MS	0.12	0.09	0.52	0.19	0.11	0.55
Br ⁻	0.36	0.05	0.48	0.41	0.09	0.51
C ₂ O ₄ ²⁻	0.78	0.01	0.16	0.77	0.01	0.17
Cu	0.52	0.12	0.52	0.52	0.11	0.52

Notes: ACE = acetate; FOR = formate; MS = methanesulphonate. Predicted/Measured fit presented is Pearson's correlation coefficient. Metals with a charge are those measured by IC, others are insoluble portions measured by ICP-MS.

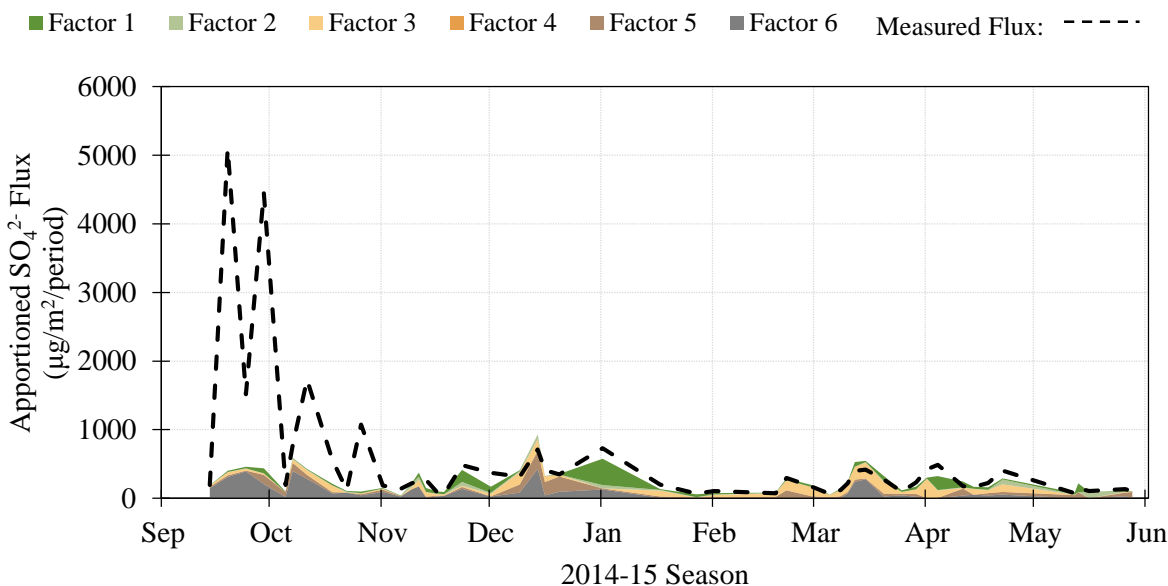


Figure S7: Predicted and measured SO₄²⁻ flux per the six-factor PMF solution.

S4 PMF Solution Sensitivity and Validation

S4.1 Solution Sensitivity and Error

The selected optimal seven-factor solution was repeated with the number of seeds increased to 500 to insure detection of the global minimum and the rotational ambiguity of this solution was then considered. For a given solution, there are several possible G and F matrices defined as rotations of the original solution. The rotation which produced the minimum value of Q was found. Furthermore, G-space plots, which compare the contribution of individual factors to each sample, were examined for the various rotation options. The factors identified by a solution should be independent, i.e., show no relationship on a G-space plot. Also, random error and rotational ambiguity of the PMF solution were quantified using a bootstrap error model with the default parameter settings: block size = 4, number of bootstraps = 50, and minimum correlation R-value = 0.6. Three error models are available with PMF5, but the bootstrap model has been recommended for data where the uncertainties are not well-known (Paatero et al., 2014).

Rotations were explored for the selected seven-factor solution with FPeak values of -1.5, -1, -0.5, 0.5, 1, and 1.5, though only the -0.5 and -1 runs were found to converge. However, G-space analysis of the base and rotated solutions showed no improvement with rotation nor did Q_{rob} values or interpretability of the solution improve; therefore, the unrotated base solution was selected. The final solution statistics were: $Q_{\text{rob}} = 355$, $Q_{\text{exp}} = 329$, $Q_{\text{rob}}/Q_{\text{exp}} = 1.08$, stability = 94%, and median predicted/measured correlation = 0.94. Residuals of all analytes were found to be normally distributed, based on PMF5's Kolmogorov-Smirnoff test, with the exception of NO_3^- and V, although both appear visually to be close to a normal distribution.

S4.2 Solution Sensitivity to Excluded Analytes

Three analytes, which matched the conditions set in section 2.4.1, were excluded from this PMF analysis for simplicity and to increase the measurement/analyte ratio: Ca^{2+} , propionate, and H^+ . While bootstrapping analysis explores the impact of removing particular measurements from the apportionment it cannot address the impact of adding additional analytes to the run. Thus, repeated PMF runs were completed including each of these analytes in turn to assess what impact they may have on the solution. All factor profiles were maintained in the augmented runs with Pearson's correlation coefficients of 0.93 or greater, with the exception of Factor 7 (Sulphate) in the H^+ run which correlated by only 0.59. Inclusion of H^+ caused MS to no longer be loaded onto Factor 7, instead distributing MS among the other factors. Since this H^+ -augmented solution caused MS to be loaded onto the clearly anthropogenic Factor 6 it was considered to be less interpretable than the base solution. However, this result may indicate that the H^+ associated with Factor 7 is mostly related to volcanic and/or smoking hills sources which were suggested to coincide with a marine biogenic SO_4^{2-} source. The time series of Factor 7 (Sulphate) was found to be fairly consistent even with the addition of H^+ with a correlation of 0.77. Therefore, the exclusion of these analytes was considered to be acceptable.

S4.3 Principal Component Analysis Validation

The relatively small number of samples available for this study was a concern, despite analyte exclusion. Therefore, a simplified supplementary principal component analysis (PCA) was completed to corroborate the PMF results. PCA has been described in detail by others (e.g., Henry et al., 1984). Briefly, PCA describes the measured data as a set of eigenvectors, termed principal components, which each describe a portion of the observed variance. These eigenvectors and their associated eigenvalues were

calculated from the correlation matrix of the measured analytes. There is no non-negativity constraint on the principal components identified by PCA as there is for PMF, nor does PCA provide quantitative factor loadings. Furthermore, PCA does not include measurement weighting by uncertainty and is therefore more sensitive to missing and below MDL values than PMF. Thus, the results of PCA are less conducive to realistic interpretations and were used only as validation of the PMF results. No rotation or error estimates were made for the PCA.

A brief PCA was completed to corroborate the PMF findings, using identical input data. The first seven principal components identified by PCA were found to explain 89% of the measured variance and agree well with the PMF factors, although a perfect correlation is not expected given the lack of non-negative constraint on the PCA results. The PCA and PMF predicted compositions agreed with Pearson's correlation coefficients of 0.39 to 0.77 and contribution time series with coefficients of 0.37 to 0.80, with the crustal and salt factors showing the best agreement. In particular, the analytes found by PMF to be dominant for each factor were generally well reflected in the PCA solution. The PCA solution found the component similar to the identified crustal and salt factors to explain the largest portion of measured variability followed by the components which resembled Factors 4 (Carboxylic Acids), 6 (Non-Crustal Metals), 3 (BC), and 5 (Nitrate), from most to least variance explained. Thus, the PCA results provided some corroboration to the PMF solution.

Table S4: PCA solution eigenvalues, eigenvectors, and contributions over campaign.

Principal Component	PC1	PC2	PC3	PC4	PC5	PC6	PC7
Eigenvalue	6.8492	3.2453	2.3119	2.0279	1.7876	0.9174	0.7215
Eigenvectors							
BC	0.19	-0.24	-0.06	-0.27	-0.28	0.33	0.01
MS	0.01	0.21	-0.47	-0.12	0.29	0.16	-0.16
ACE	0.11	0.16	-0.39	0.15	-0.39	-0.14	-0.10
FOR	0.16	-0.06	-0.26	0.46	-0.19	-0.23	0.21
Cl-	0.18	0.38	0.30	-0.03	-0.14	0.11	-0.01
Br-	0.06	0.32	0.11	0.01	-0.48	-0.04	-0.05
NO3-	0.14	-0.17	-0.06	-0.35	-0.04	-0.33	0.63
SO4=	0.06	0.24	-0.45	-0.23	0.28	0.15	0.03
C2O4=	0.29	0.08	0.25	-0.18	0.14	-0.07	0.07
Na+	0.20	0.38	0.29	-0.05	-0.04	0.11	-0.06
NH4+	0.23	0.14	-0.29	-0.11	-0.32	-0.10	0.02
K+	0.20	0.26	0.06	-0.19	0.23	-0.35	0.18
Mg++	0.27	0.32	-0.05	0.12	0.21	0.13	0.04
IS Al	0.32	-0.11	0.02	0.31	0.13	0.08	0.12
IS V	0.33	-0.15	0.03	0.22	0.14	0.10	0.08
IS Cu	0.20	-0.09	0.04	-0.02	0.15	-0.61	-0.58
IS As	0.31	-0.19	0.03	-0.06	-0.04	0.28	-0.19
IS Se	0.31	-0.11	-0.01	0.34	0.14	0.07	0.01
IS Sb	0.20	-0.24	-0.07	-0.33	-0.13	-0.02	-0.28
IS Pb	0.31	-0.21	0.00	-0.20	-0.03	0.07	-0.02
Component Contribution							
9/14/2014	-1.777	-0.381	0.1027	0.1039	0.804	-0.159	0.0959
9/19/2014	-0.004	3.7118	-5.881	-1.286	3.0331	1.7229	-0.745
9/24/2014	-0.788	1.2373	-1.006	-0.222	1.3064	0.181	0.0384
9/29/2014	1.2476	3.7531	-3.676	-2.13	1.9661	-0.351	1.2667
10/5/2014	-2.193	-0.275	0.4071	0.1777	0.7021	-0.678	0.6511
10/7/2014	2.2723	-1.207	-0.507	-1.96	0.0395	-2.298	-0.913
10/11/2014	1.733	-0.062	-3.131	-0.257	-1.023	-0.633	-0.419
10/18/2014	-1.281	-0.188	-0.087	-0.135	-0.186	0.1674	0.0714
10/22/2014	-1.487	-1.035	0.6771	0.8351	0.936	-0.081	-0.573
10/26/2014	-1.906	-0.076	0.251	-0.012	0.9286	0.1673	0.0169
11/1/2014	-1.749	-0.737	0.3842	0.4436	0.4989	-0.195	0.0619
11/6/2014	-2.915	-0.546	0.4566	0.7499	0.5667	0.1511	-0.067
11/9/2014	2.1621	-1.657	0.8076	1.5717	1.8824	0.07	-0.924
11/11/2014	2.9388	-1.462	0.6757	-0.003	0.687	0.6053	-1.397
11/13/2014	-1.482	0.5422	0.2844	0.0877	-0.236	0.1044	0.1716
11/16/2014	-1.977	-0.407	0.8266	0.6004	0.7078	0.0604	-0.303

Table S4 (continued): PCA solution eigenvalues, eigenvectors, and contributions over campaign.

Principal Component	PC1	PC2	PC3	PC4	PC5	PC6	PC7
Component Contribution (continued)							
11/18/2014	-2.14	-0.214	1.0614	0.3649	0.6969	0.1541	-0.261
11/23/2014	4.9011	0.9812	2.7053	0.6318	1.937	0.6514	-0.359
12/1/2014	-1.071	0.5607	1.0837	0.5232	0.7537	0.7392	0.0061
12/9/2014	0.591	-1.722	-0.206	-0.971	-0.662	0.5508	0.8866
12/14/2014	8.4113	-4.899	0.1763	-3.536	0.0949	0.1842	1.1751
12/16/2014	-0.962	-1.26	-0.938	-0.967	-1.103	-0.808	1.1113
12/20/2014	-0.641	-1.883	-0.01	-2.218	-0.131	-1.548	1.8145
1/1/2015	7.3992	5.5857	4.206	-0.591	1.7431	-0.505	0.1849
1/17/2015	-1.545	-0.573	0.5883	0.3957	0.5222	0.3855	0.181
1/27/2015	-2.345	-0.138	0.9806	0.8369	0.9214	0.3837	0.0971
2/1/2015	-1.817	-0.558	0.7511	0.9225	0.743	0.4697	0.1679
2/18/2015	-2.603	-0.716	0.454	0.5469	0.3575	0.3799	0.1046
2/21/2015	-0.755	-0.418	0.1606	-0.832	-0.121	-0.19	1.1472
2/28/2015	-1.797	-0.484	0.4269	-0.143	-0.027	0.7385	0.2814
3/5/2015	-2.796	-0.738	0.6729	0.4513	0.6189	0.3021	-0.047
3/8/2015	-2.203	-0.557	0.5125	0.1383	0.0826	0.4174	0.2675
3/10/2015	-0.742	-1.469	-0.429	-0.913	-0.981	0.2232	-0.841
3/12/2015	1.4551	-0.538	-0.135	-1.555	-2.43	1.136	-1.395
3/15/2015	1.5565	-1.786	-0.363	-1.538	-1.895	1.7849	-1.537
3/20/2015	0.8284	0.579	0.3942	-0.349	-1.188	0.6161	0.2933
3/25/2015	-1.673	-0.078	0.2275	0.4618	-0.253	0.0499	0.0304
3/29/2015	-1.073	1.1995	0.1091	0.3616	-2.274	-0.089	-0.022
4/1/2015	-0.555	0.06	-0.389	0.0803	-2.365	0.664	-0.397
4/4/2015	1.6846	4.9962	0.7832	0.8217	-3.982	0.5339	-0.388
4/11/2015	0.2854	1.1339	1.0431	-0.477	-0.995	-0.165	0.8896
4/14/2015	-0.63	1.0493	-1.468	0.1646	-2.183	0.0817	-0.495
4/18/2015	-1.413	0.2557	0.1022	0.1346	0.2222	0.4202	-0.135
4/22/2015	3.7308	-1.593	-0.156	1.0841	1.2759	1.1381	-0.506
5/12/2015	-1.181	0.8304	0.1325	0.5419	-0.57	-1.295	0.9403
5/13/2015	0.0918	3.0195	1.1441	-0.173	-1.556	-1.032	0.8812
5/16/2015	6.7261	-1.775	-3.354	7.1336	-0.942	-0.646	1.2897
5/26/2015	-0.374	0.0607	-0.606	0.1098	0.4894	-4.202	-2.983
5/28/2015	-2.139	-0.125	-0.246	-0.007	0.5846	-0.359	0.5833
Comparison with PMF Results - Pearson's Correlation Coefficient							
Similar Factor	2	1	4	6	7	3	5
Composition	0.68	0.77	-0.50	-0.39	0.55	0.40	0.59
Contribution	0.80	0.67	-0.54	-0.49	0.37	0.39	0.53

Notes: Since PCA does not enforce a positive factor, the resultant factors may be arbitrarily positive or negative. The Pearson's correlation coefficients should be evaluated in terms of absolute magnitude, not sign.

Supplemental References

Henry, R. C., Lewis, C. W., Hopke, P. K., and Williamson, H. J.: Review of receptor model fundamentals, *Atmos. Environ.* (1967), 18 (8), 1507–1515, doi:10.1016/0004-6981(84)90375-5, 1984.

Macdonald, K. M., Sharma, S., Toom, D., Chivulescu, A., Hanna, S., Bertram, A. K., Platt, A., Elsasser, M., Huang, L., Tarasick, D., Chellman, N., McConnel, J., Bozem, H., Kunkel, D., Ying Duan, L., Evans, G. J., and Abbatt, J. P. D.: Observations of atmospheric chemical deposition to high Arctic snow, *Atmos. Chem. Phys.*, doi:10.5194/acp-17-5775-2017, 2017.

Norris, G., Duvall, R., Brown, S., and Bai, S.: EPA Positive matrix factorization (PMF) 5.0 fundamentals and user guide, U.S. Environmental Protection Agency, 2014.

Paatero, P., Eberly, S., Brown, S. G., and Norris, G. A.: Methods for estimating uncertainty in factor analytic solutions, *Atmospheric Measurement Techniques*, 7 (2008), 781–797, doi:10.5194/amt-7-781-2014, 2014.